

Accepted Manuscript

Title: NiO-doped Au/Ti-powder: A Catalyst with Dramatic Improvement in Activity for Gas-phase Oxidation of Alcohols

Author: Guofeng Zhao Huanyun Hu Zheng Jiang Shuo Zhang Yong Lu



PII: S0926-860X(13)00403-1
DOI: <http://dx.doi.org/doi:10.1016/j.apcata.2013.07.005>
Reference: APCATA 14321

To appear in: *Applied Catalysis A: General*

Received date: 13-3-2013
Revised date: 29-6-2013
Accepted date: 3-7-2013

Please cite this article as: G. Zhao, H. Hu, Z. Jiang, S. Zhang, Y. Lu, NiO-doped Au/Ti-powder: A Catalyst with Dramatic Improvement in Activity for Gas-phase Oxidation of Alcohols, *Applied Catalysis A, General* (2013), <http://dx.doi.org/10.1016/j.apcata.2013.07.005>

This is a PDF file of an unedited manuscript that has been accepted for publication. As a service to our customers we are providing this early version of the manuscript. The manuscript will undergo copyediting, typesetting, and review of the resulting proof before it is published in its final form. Please note that during the production process errors may be discovered which could affect the content, and all legal disclaimers that apply to the journal pertain.

**NiO-doped Au/Ti-powder: A Catalyst with Dramatic Improvement in Activity
for Gas-phase Oxidation of Alcohols**

Guofeng Zhao^a, Huanyun Hu^a, Zheng Jiang^b, Shuo Zhang^b and Yong Lu^{*a}

^a Shanghai Key Laboratory of Green Chemistry and Chemical Processes, Department of Chemistry,
East China Normal University, Shanghai 200062, China.

^b Shanghai Synchrotron Radiation Facility, Shanghai Institute of Applied Physics, Chinese
Academy of Sciences, Shanghai 201204, China.

* Corresponding author: Yong Lu,

Shanghai Key Laboratory of Green Chemistry and Chemical Processes, Department of Chemistry,
East China Normal University, Shanghai 200062, China.

Tel.: +86-21-62233424; Fax: +86-21-62233424;

Email address: ylu@chem.ecnu.edu.cn (Y. Lu).

Abstract

An active and stable NiO@Au/Ti-powder catalyst, which can be obtained by doping Au/Ti-powder (Au: 35-40 nm) with NiO, has been developed for the gas-phase oxidation of alcohols. Gold particles are found to be partially covered with tiny NiO segments to form specific NiO@Au ensembles thereby leading to a dramatic conversion improvement from only ~5% (without NiO doping) to ~94% for the benzyl alcohol oxidation at 280 °C. Additionally, the selective oxidation of cyclopropyl carbinol can proceed over this catalyst at 280 °C with a selectivity of 94% and a conversion of 72-80% throughout the entire 300 h test. The hybrid active-sites, Ni₂O₃-Au⁺, on the NiO@Au ensemble are identified using X-ray photoelectron spectroscopy (XPS) and X-ray absorption spectroscopy (XAS).

Keywords: gold catalyst, NiO, interface, active site, alcohol oxidation, aldehyde

1. Introduction

Selective oxidations of alcohols to carbonyl compounds are some of the most important processes in organic chemistry, both in laboratory and in industrial manufacturing [1-9]. However, the use of various toxic and expensive stoichiometric inorganic oxidants (notably Cr reagents) and volatile organic solvents in the existing oxidation processes causes serious problems in product separation and environmental issues, obviously conflicting the atom-economical concept of green chemistry [1-9]. Therefore, there should be a paradigm shift away from traditional approaches, aimed at using atmospheric air and recyclable heterogeneous catalysts under solvent-free conditions [1-9].

Supported gold catalysts have been extensively studied for the aerobic oxidation of alcohols [1-9]. Generally, their activity is related to the size of gold nanoparticles (Au NPs) [2,4,10-13], the chemical state of the gold [14-16], the support properties [17-21], and the gold-support interactions [22]. The small Au NPs (<5 nm) has been widely accepted to be essential for good catalytic activity [12], and the other factors are all discussed based on the use of the small Au NPs. Recently, however, some reports disclosed the occurrence of the opposite behavior, which warrants the reconsideration of this fundamental belief. For example, catalysts comprising a transition metal oxide deposited on a single crystal of gold, such as $\text{CeO}_2/\text{Au}(111)$ [23,24] and $\text{TiO}_2/\text{Au}(111)$ [25], are not even nano-scale but still show higher catalytic activity than Au NPs supported on oxides. Therefore, particle size is not the only parameter that strongly affects the activity of these catalysts. There should be another model to explain the excellent activity displayed by the large gold particles in some reactions.

More recently, NiO@Au ensembles (*i.e.*, partial coverage of 20-30 nm Au particles with NiO

segments) have been reported by our group, which are highly active and selective for the gas-phase oxidation of alcohols [26-28]. Guided by our previous results, we attempted to place NiO@Au ensembles on a suitable support for obtaining a practical and versatile catalyst with high activity/selectivity, good stability and high heat conductivity. Because gas-phase alcohol oxidation reactions are highly exothermic, it is desirable to endow the catalyst with high heat conductivity for rapidly dissipating reaction heat from the catalytic reactor bed. The oxide-supported catalysts demonstrated good low-temperature activity, but their poor heat conductivity causes hotspots to form in the reaction bed [3]. Therefore, metal support is a reasonable alternative. Compared to the metallic Ni [26-28] and Cu [29,30] microfibrillar supports, Ti powder was a good support candidate because of its low price, low coking activity, high oxidation-/acid-corrosion resistance, inert behavior toward the alcohol oxidation, and relatively high heat conductivity. In order to further elucidate the activity origin of the NiO@Au/Ti-powder catalyst, X-ray photoelectron spectroscopy (XPS) and X-ray absorption spectroscopy (XAS) were employed to reveal the active-sites on the NiO@Au ensembles.

2. Experimental

2.1 Catalyst preparation

The Au/Ti-powder catalyst (5 wt% Au, denoted as Au-5/Ti) was prepared by impregnating Ti-powder (200-300 mesh, Alfa Aesar) with H₂AuCl₄ solution, followed by calcination at 300 °C in air for 4 h. Au-5/Ti catalyst was then impregnated with aqueous NiCl₂ solution (to 1 wt% NiO) and calcined at 400 °C in air for 4 h, which transformed the NiCl₂ into NiO. By doing so, a NiO-doped Au-5/Ti catalyst was obtained and denoted as NiO-1@Au-5/Ti-Cl. NiO-1@Au-5/Ti-N and NiO-1@Au-5/Ti-C catalysts were also prepared by using this method except that Ni(NO₃)₂ and

Ni(Ac)₂ were used as precursors, respectively. Catalysts with different Au and NiO loadings were prepared by following the same procedure and simply tuning the amount of HAuCl₄ and nickel salts in the corresponding solutions.

Additionally, the NiO-1/Ti-Cl catalyst was prepared by impregnating Ti-powder with a NiCl₂ solution to NiO loading of 1 wt%, followed by calcination at 400 °C in air for 4 h. The Au-5@NiO-1/Ti-Cl catalyst was prepared by impregnating the NiO-1/Ti-Cl catalyst with a solution of HAuCl₄ to Au loading of 5 wt%, followed by calcination at 300 °C in air for 4 h.

2.2 Catalyst characterization

The catalysts were characterized with X-ray diffraction (XRD, Rigaku Ultima IV diffractometer (Cu K α)), scanning electron microscopy (SEM, Hitachi S-4800) equipped with an energy dispersive X-ray analysis (EDX) unit (Oxford, UK), and transmission electron microscopy (TEM, JEOL-JEM-2010 instrument at 200 kV). XPS were recorded on a VG EscaLab 220i spectrometer, which used a standard Al K α X-ray source (300 W) and an analyzer pass energy of 20 eV. All binding energies are referenced to the C1s line at 284.9 eV. XAS data of the Au L^{III}-edge (11,919 eV) and Ni K-edge (8350 eV) were collected in transmission mode on the BL14W1 beam line of the Shanghai Synchrotron Radiation Facility (SSRF). The typical electron beam energy was 3.5 GeV, and the current was 300 mA. A cryogenically cooled double-crystal Si (111) monochromator was used to minimize the harmonics. The extended X-ray absorption fine structure (EXAFS) spectra were analyzed with the ATHENA software. The loading of gold for all of the samples was determined by inductively coupled plasma atomic emission spectrometry (ICP-AES) on a Thermo Scientific iCAP 6300 ICP spectrometer.

2.3 Reactivity tests

The gas-phase oxidation of alcohols was performed on a fixed-bed quartz tube reactor (700 mm length by 16 mm inner diameter) under atmospheric pressure as described previously [31,32]. Catalyst used in each test was 0.3 g (200-300 mesh). Alcohols were fed continuously via a high-performance liquid pump in parallel with O₂ (oxidant) and N₂ (diluted gas of 100 ml/min) feeding, which used calibrated mass flow controllers, into the reactor under steady-state temperature conditions. The weight hourly space velocity (WHSV) was calculated by dividing the mass flow rate of the alcohol feedstock by the catalyst mass. The effluent was cooled using an ice-salt bath (-15 °C) to condense the vapors for analysis using a Shimadzu-2014 gas chromatography-flame ionization detector (GC-FID) with a 60 m HP-5ms capillary column. The gas-phase products, such as H₂, CO_x, and C1-C3 hydrocarbons, were analyzed using an HP-5890 GC with a thermal conductivity detector (TCD) and a 30 m AT-plot 300 capillary column. The reproducibility of the conversion and selectivity of the product was high and the error range was ± 0.2%. A carbon mass balance close to 100% was achieved.

3 Results and discussion

3.1 Highly active NiO@Au ensembles

HAuCl₄ and NiCl₂ were chosen as the preferred precursors in the fabrication of the NiO@Au ensembles because of the previously reported galvanic exchange reaction that yielded metallic gold particles and NiCl₂ from HAuCl₄ and Ni fiber [26,27]. First, we prepared an Au/Ti-powder catalyst (5 wt% Au; denoted as Au-5/Ti) by impregnation of Ti-powder with a HAuCl₄ solution and subsequent calcination at 300 °C in air for 4 h. Specific surface area of the Au-5/Ti catalyst is only 0.2 m²/g, close to that (0.1 m²/g) for the Ti-powder support itself (Table S1). SEM (Fig. 1A), XRD

(Fig. 1B) and TEM (Fig. 1C) measurement results clearly showed that the HAuCl_4 decomposed to form metallic gold particles on Ti-powder surface. As shown in Table 1 and Fig. S1, gold particles of the Au-5/Ti catalyst, with size around 35-40 nm, are much larger than the small Au particles (<5 nm) desired for achieving good catalytic activity [12]. When subjected to oxidation of benzyl alcohol, not surprisingly, the Au-5/Ti catalyst delivered very low benzyl alcohol of <6%, comparable to the Ti-powder support itself (entries 1,2 in Table 1). Subsequently, the Au-5/Ti catalyst was impregnated with NiCl_2 solution to a NiO loading of 1 wt%, followed by calcination at 400 °C. The XRD patterns demonstrated that NiCl_2 was transformed into NiO, which co-existed with Au particles to produce a NiO-doped Au/Ti catalyst (denoted as NiO-1@Au-5/Ti-Cl; Fig. 2, Scheme S1). The EDX results indicated that the Ni was on the surface of the Au particles (Fig. S2). Most interestingly, NiO-doping resulted in a dramatic improvement in activity for the gas-phase oxidation of benzyl alcohol. Benzyl alcohol conversion of only 5.2% was observed over the Au-5/Ti (entry 2 in Table 1), but a high conversion of 93.7% was obtained over the NiO-1@Au-5/Ti-Cl (entry 3 in Table 1). Note that the specific surface area of the catalysts almost remained unchanged (*i.e.*, 0.2 m²/g; Table S1) with or without NiO-doping. Thus, the dramatic conversion promotion assignment to the surface area change can be reasonably ruled out. For reference, NiO-1/Ti-Cl was prepared and, when subjected to the benzyl alcohol oxidation, yielded a conversion of only 2.3% (entry 4 in Table 1). Clearly, the singular use of Au or NiO particles was ineffective for the gas-phase oxidation of alcohols.

Fig. 1D and Fig. S3 show the TEM images of the NiO-1@Au-5/Ti-Cl catalyst. Clearly, large Au particles (~40 nm) were partially covered with small NiO segments to form NiO@Au ensembles. Additionally, when we placed 5 wt% Au onto the NiO-1/Ti-Cl catalyst, the resultant

Au-5@NiO-1/Ti-Cl catalyst did not show dramatic activity improvement yet (entry 5 in Table 1). This catalyst delivered a benzyl alcohol conversion of only 21.1%, much lower than that (93.7%) for the NiO-1@Au-5/Ti-Cl. Note that the Au-5@NiO-1/Ti-Cl catalyst was obtained by placing NiO (1wt%) firstly onto the Ti-powder support to form NiO-1/Ti-Cl and subsequently depositing gold (5wt%) on the NiO-1/Ti-Cl. By using this method, it is difficult to form the NiO@Au ensembles when compared to the method for the NiO-1@Au-5/Ti-Cl catalyst preparation. The above results indicated that the formation of the NiO@Au ensembles is essential for the high activity of the Au-5@NiO-1/Ti-Cl catalyst. This observation is in agreement with our previous report for the Au/Ni-fiber catalyst system [26,27].

3.2 Influences of nickel precursors, loadings of gold and nickel

However, we wonder whether it is only method for forming the NiO@Au ensembles use NiCl₂ as the precursor. To address this question, two additional catalysts were prepared by impregnating Au-5/Ti catalysts with Ni(Ac)₂ and Ni(NO₃)₂ solution (to 1 wt% NiO) and subsequently calcining at 400 °C in air for 4 h. These two new catalysts, denoted as NiO-1@Au-5/Ti-C and NiO-1@Au-5/Ti-N, were examined in the gas-phase oxidation of benzyl alcohol. As expected, both catalysts showed activity comparable to that of the NiO-1@Au-5/Ti-Cl catalyst, yielding benzyl alcohol conversions of 92.1% and 94.6% (entries 6, 7 in Table 1). These results indicated that upon fabricating the special NiO@Au ensembles, the corresponding catalysts always show excellent activity in the reaction, regardless of the identity of the nickel precursors (Fig. S4). It should be noticeable that our catalysts were still active at lower reaction temperatures. Over the NiO-1@Au-5/Ti-N catalyst, for instance, the benzyl alcohol conversion declined from 94.6% to 86.0% as the temperature was decreased from 280 to 230 °C (entries 7-10 in Table 1). An

acceptable conversion of 63.5% could still be obtained when the temperature was decreased to 220 °C (entries 11 in Table 1).

In addition, the Au and NiO loadings of the NiO@Au/Ti-Cl catalysts could be tuned within a large range without risking the degradation of their catalytic performance (Fig. 3). The influence of NiO loading on the catalyst performance was investigated from 0.3 to 7 wt%, with the Au loading maintained at 5 wt% (Fig. 3A). Benzyl alcohol conversion was increased from 54.2 to 93.7% along with the increase of NiO loading from 0.3% to 1 wt%, and then remained almost unchanged until to 4 wt%. Further increasing NiO loading to 5 wt% and then up to 7 wt% led to a decrease in the benzyl alcohol conversion to 79.1% and then 77.1%. By setting the Au/NiO weight ratio of 5, the effect of gold loading was investigated from 1 to 5 wt%, with the results as shown in Fig. 3B. Clearly, the catalytic activity almost showed no alteration until the gold loading was reduced to 3 wt% (corresponding NiO loading: 0.6 wt%). Note that the reduction of the Au loading is particularly desirable for practical applications.

3.3 Selectivity oxidation reactivity for other alcohols

The NiO-1@Au-5/Ti-Cl catalyst was also tested for the oxidation of a range of straight-chain (1-octanol, 2-octanol), benzylic (1-phenylethanol, 2-phenylethanol), cyclic (cyclohexanol) and polynary (1,2-propanediol) alcohols, with the results as summarized in Table 2 and Table S2. Conjugated aromatic alcohols could be oxidized to the corresponding conjugated aldehydes or ketones faster than the aliphatic alcohols. At equivalent selectivity, for example, a high conversion of 95.3% could be obtained for the 1-phenylethanol oxidation at 300 °C but it was only 51.2% for the 2-phenylethanol oxidation even at 340 °C. Similarly, the straight-chain octanol was less reactive than the 1-phenylethanol. Interestingly, the primary linear aliphatic octanol was more reactive than

the secondary counterparts: 51.9% conversion for 1-octanol at 300 °C vs. 23.4% conversion for 2-octanol at 360 °C. Cyclohexanol could be selectively oxidized to cyclohexanone (a key raw material in the synthesis of many useful chemicals, such as caprolactam for nylon 6 and adipic acid for nylon 66) at a conversion of 67.8% with a selectivity of 97.4% at 340 °C. For the 1,2-propylene glycol oxidation, it is in general favorable to form hydroxyketone rather than methyl glyoxal. Notably, our NiO-1@Au-5/Ti-Cl catalyst delivered a good methyl glyoxal selectivity of 71.0% and a high conversion of 91.6%.

3.4 Reaction stability tests

Stability is a very important practical consideration for a heterogeneous catalyst. For the benzyl alcohol oxidation at 280 °C, the NiO-1@Au-5/Ti-Cl catalyst delivered a single-run lifetime as long as 130 h with a very steady catalytic reactivity (conversion: 88-94%, selectivity: 99%; Fig. 4A), which showed much better activity and selectivity over time than the other reported catalysts [1,3]. This single run lifetime over the NiO-1@Au-5/Ti-Cl catalyst is comparable to the 140 h lifetime demonstrated by our previously reported Au-4/Ni-fiber-300 catalyst [26,27]. In this 130-h single run, the equilibrium inversion rate of benzyl alcohol was 18.4 g per hour per gram of NiO-1@Au-5/Ti-Cl and a benzaldehyde yield of 2.3 kg per gram NiO-1@Au-5/Ti-Cl (or 46 kg per gram of Au) could be achieved. Additionally, the liquid effluent could be automatically separated into a water phase and a clear pale yellow organic phase, which contained predominantly benzaldehyde (CO, CO₂, benzene, toluene and benzoic acid were formed in trace amounts).

As previously noted, the lifetime of Au/SiO₂ catalyst is only 70 h using a lower WHSV of 10 h⁻¹ at 315 °C, with the selectivity of 90-100% and the conversion in the wider range of 50-75% [1,3]. The decay of the catalytic behavior was ascribed to the formation of a pitch-dark deposition caused

by the weak heat transfer ability. Whereas the K-Cu-TiO₂ shows a very high conversion of 99% at 210 °C (bed temperature: 227 °C) using a very low WHSV of 0.6 h⁻¹, the reported lifetime of it is only 50 h and its throughput is extremely low [33].

We then conducted a longer-term test using cyclopropyl carbinol over the NiO-1@Au-5/Ti-Cl catalyst. At 280 °C, the conversion of cyclopropyl carbinol was ~80% and remained unchanged within the first 230 h run, using a WHSV of 20 h⁻¹ and an O₂/hydroxyl molar ratio of 0.6. After that, the conversion was decreased slowly to ~72% within another 70 h time-on-stream. Note that the selectivity to cyclopropyl formaldehyde was always ~94% throughout the entire 300-h test (Fig. 4B). In this 300-h single run, the average conversion of cyclopropyl carbinol was approximately 77%. Cyclopropyl formaldehyde could be obtained at a rate of 15.4 g per hour over per gram NiO-1@Au-5/Ti-Cl, and a yield of 4.6 kg per gram NiO-1@Au-5/Ti-Cl (or 92 kg per gram Au) could be achievable. After 300-h oxidation of cyclopropyl carbinol, the size of Au particles and the NiO@Au ensemble structure were retained well (Fig. S5), which indicated that the catalyst is stable and robust.

3.5 Identification of active sites

3.5.1 XPS studies

As is well known, a reaction takes place on the active sites at the catalyst surface. Therefore, revealing the active sites is particularly desirable for elucidation of the activity improvement associated with the formation of NiO@Au ensembles. To accomplish this goal, surface-sensitive XPS technique was used to track the evolution behavior of the surface chemical composition for the NiO-1@Au-5/Ti-Cl catalysts after undergoing a specifically designed three-stage reaction procedure in the tubular reactor at 280 °C: the reaction was carried out with alcohol/O₂ mixture

feedstock, subsequently with sole alcohol by cutting-off O₂ and then re-feeding O. Table 3 and Fig. 5 summarized the XPS results for the NiO-1@Au-5/Ti-Cl samples collected at the each stage of the above reaction treatment procedure. On the sample a (Table 3, undergoing reaction with alcohol/O₂ mixture feedstock for 0.5 h), apart from Au⁰ (Au4f (7/2): 84.0 eV) and NiO (Ni2p: 854.4 eV; O1s: 529.7 eV), not only were a large amount of Ni₂O₃ specimens (Ni2p: 856.2 eV; O1s: 531.8 eV) formed but a considerable number of Au⁺ specimens were also clearly detected with the Au4f (7/2) peak at 84.8 eV (Fig. 5-a). On such surface, the Au⁺ surface content to total surface gold atoms was 37.0% and surface Ni₂O₃ content to total surface nickel oxides was 77.0% with the surface Au⁺/Ni³⁺ ratio of 1/14 (Table 3, Table S3).

Interestingly, when the sample a reacted with benzyl alcohol alone at 280 °C for 15 min, which was achieved by cutting off O₂ from the stream (Fig. 5-b, named sample b), the Au⁺ surface content was decreased significantly from 37.0% to less than 4% while the surface Ni₂O₃ content was decreased from 77.0% to 60.0% by correspondingly transferring to NiO (surface NiO content was increased from 23.0% to 40.0%; Table 3). As a result, the benzyl alcohol conversion showed a sharp reduction from 94% to 2%. After the sample b reacted with mixture of benzyl alcohol and O₂ by retrieving the O₂ feeding at 280 °C for 10 min (*i.e.*, sample c), the surface Au⁺ and Ni₂O₃ contents were recovered, nearly reaching the level of the sample a, and this was accompanied by a significant increase in benzyl alcohol conversion to 88% (Fig. 5-c, Table 3). Unlike the high-low-high evolution behavior of the surface Au⁺ and Ni₂O₃ content, the surface TiO₂ content remained at 36.0% in the whole process of with-without-with O₂ reaction procedure (Fig. S6, Table S3).

3.5.2 XAS studies

As a sensitive technology to probe the local geometry and identify the oxidation states of metallic particles [34-36], the X-ray absorption near-edge structure (XANES) was also employed to study the three catalyst samples (same as in above XPS studies) at the Au L₃ and Ni K edge, with the results as shown in Fig. 6 and Fig. 7. The characteristic high-low-high evolution behavior for the Au⁺ and Ni₂O₃ specimens was observed again along with the respective with-without-with O₂ presence in the reaction feed gas, which is in good agreement with the XPS results. The sample a showed a higher intensity of whiteline than that of the Au foil (Fig. 6A-a,b) and a similar XANES with the reported mixture of Au⁺ complexes and Au⁰ particles [36]. This observation definitely indicated that Au⁺ formed in the NiO@Au ensembles. Interestingly, as the sample a underwent the reaction for 15 min with only benzyl alcohol in the absence of O₂, the whiteline intensity exhibited a slight decrease and the resulting XANES was similar with that of Au foil. This indicated that the Au⁺ disappeared almost completely (Fig. 6A-b,c). After feeding O₂ again for 10 min (*i.e.*, sample c), the whiteline intensity increased slightly while an XANES similar with that for the sample a appeared again. This result indicated that the amount of Au⁺ was re-increased nearly close to that for the sample a (Fig. 6A-c,d). This trend could also be observed in the changes in Au-O coordination over the course of these three samples (Fig. 6B, Table S4). An Au-O coordination was present at a distance of 1.7 Å in the sample a (Fig. 6B-a), being consistent with the previously reported results [37]. In the sample b, the Au-O coordination almost disappeared and the data were similar to those of the Au foil (Fig. 6B-b,c). In the sample c, not surprisingly, the Au-O coordination increased once again to be close to that for the sample a (Fig. 6B-a,d).

Additionally, the whiteline intensity of the XANES at the Ni K edge also showed high-low-high

changes along with the respective with-without-with O₂ reaction procedure (Fig. 7A). For the sample a, the whiteline intensity at 8350 eV was slightly lower than that of the Ni₂O₃ (Fig. 7A-a,b) because the Ni species in the sample a was a mixture of NiO and Ni₂O₃. Along with the O₂ cutting off and subsequently re-feeding, the whiteline intensity at 8350 eV became slightly lower for the sample b (Fig. 7A-c) than that for the sample a (Fig. 7A-b) and then retrieved nearly close to that for the sample a (Fig. 7A-d). For reference, the XANES of the NiO was also included and it exhibited a much lower whiteline intensity than Ni₂O₃ (Fig. 7A-a,e). In addition, the changes in Ni-O coordination across these three samples also demonstrated the same high-low-high trend (Fig. 7B). The Ni-O coordination was presented at a distance of 1.6 Å in the sample a, which is similar to the Ni-O coordination of Ni₂O₃ [36] (Fig. 7B-a,b). In comparison with the sample a, the Ni-O coordination was decreased slightly (Fig. 7B-c) in the sample b due to the O₂ cutting off. However, after re-feeding O₂ the Ni-O coordination in the sample c was increased again close to the level of the sample a (Fig. 7B-b,d). Combining the XANES results with the information from the XPS studies, it was rational to infer that the high-low-high changes of the absorption intensity at 8350 eV was attributable to the high-low-high change of Ni₂O₃ content.

3.5.3 Ni₂O₃-Au⁺ hybrid active sites

The Au-5/Ti and NiO-1/Ti-Cl catalysts delivered a very low activity for the benzyl alcohol oxidation (<5%) and, even when they were physically mixed, the benzyl alcohol conversion still remained very low (only 4.3%, entry 12 in Table 1). However, the NiO-1@Au-5/Ti-Cl (-N, and -A) catalysts with the formation of NiO@Au ensembles all delivered much higher benzyl alcohol conversion of >90% at 280 °C (Table 1, Fig. 1D, Fig. S4). These results indicated that the co-existence of NiO and Au in the form of NiO@Au ensembles, in contrast to being physically

mixed, was essential for the high activity for the alcohol oxidation. Additionally, the NiO@Au ensembles were analyzed by TEM and the NiO-Au interface was clearly detected (Fig. S7A-B). The EDX results (Fig. S7C) indicated the presence of elemental Au and Ni in the cycled parts in Fig. S7A-B. As noted previously, the interface between NiO and Au is essential for high alcohol oxidation activity [38]. As shown in Fig. S7A-B, only the lattice fringe of NiO was detected while the lattice fringe of Au could not be detected because the gold particle was so large. Moreover, the lattice fringe of the NiO segments was slightly bent rather than the linear lattice fringe of bulk NiO, which might be a result of the formation of NiO@Au ensemble structure.

The Au-5/Ti, NiO-1/Ti-Cl, and NiO-1@Au-5/Ti-Cl catalysts were characterized by XPS, with the results as summarized in Table S5. Interestingly, the Au⁺ content in the Au-5/Ti and the Ni₂O₃ content in the NiO-1/Ti-Cl were very low, while both was increased greatly in the NiO-1@Au-5/Ti-Cl catalyst. The large difference in the Au⁺ and Ni₂O₃ contents in these catalysts was associated with the pronounced difference in the benzyl alcohol conversion (Au-5/Ti: 5.2%, NiO-1/Ti-Cl: 2.3%, and NiO-1@Au-5/Ti-Cl: 93.7%; Table 1). This observation indicated that the Au⁺ and Ni₂O₃ were important to the catalyst performance. Additionally, in the with-without-with O₂ reaction procedure, over the NiO-1@Au-5/Ti-Cl catalyst the benzyl alcohol conversion also exhibited high-low-high evolution behavior (*e.g.*, 94% vs. 2% vs. 88%; Table 3).

The above XPS and XANES results clearly showed the high-low-high surface contents of Au⁺ and Ni₂O₃ but not NiO (Fig. 6 and Fig. 7). This observation was clearly associated with the high-low-high evolution behavior of the benzyl alcohol conversion in the with-without-with O₂ reaction procedure. Accordingly, hybrid active-sites of Ni₂O₃-Au⁺ was defined, which is the origin of the dramatic activity improvement associated with the formation of the NiO@Au ensembles.

With the sharp high-low-high evolution behavior of the benzyl alcohol conversion, the Au⁺ surface content also showed the same sharp high-low-high change (*e.g.*, 37.0% vs. 3.4% vs. 33.0%; Table 3). Meanwhile, the surface Ni₂O₃ exhibited a similar high-low-high content shift (*e.g.*, 77.0% vs. 60.0% vs. 73.0%; Table 3), but the change was smaller when compared with the benzyl alcohol conversion and the Au⁺ surface content. Clearly, there was a stronger relationship between the benzyl alcohol conversion and the Au⁺ surface content, indicating that the Au⁺ might work as the main active species for the alcohol oxidation with the Ni₂O₃ as an assisting species. It has been reported in some studies that the Ni₂O₃ specimens play a key role not only in promoting the formation of Au⁺ species and stabilizing them but also in acting as a surface-active-oxygen supplier [39,40].

By nature, it could be proposed that Ni₂O₃ could not only increase and stabilize the Au⁺ located at the NiO-Au interface but also could adsorb oxygen molecules into its oxygen vacancies and activate the adsorbed molecular oxygen, which resulted in the active oxygen species. Such oxygen species could be transferred onto the Au⁺ sites to react with alcohol while opening a new oxygen vacancy for the next catalytic cycle.

4 Conclusions

The interesting date-cake-like active NiO@Au ensembles, which are characteristic of the partial coverage of the large Au particles with small NiO segments, are successfully fabricated from various precursors and are found to be highly active in the gas-phase oxidation of alcohols. In addition, the Au and NiO loadings can be tuned within a large range without any degradation of the catalytic performance of the NiO@Au ensembles. Notably, with the high-low-high changes in the benzyl alcohol conversion following an operation with-without-with O₂ in the reactant stream, the

high-low-high surface content of Au^+ is associated with an analogous change with Ni_2O_3 but not NiO . The hybrid active-sites of $\text{Ni}_2\text{O}_3\text{-Au}^+$ are defined accordingly, which is the origin for the low-temperature activity. The NiO@Au ensembles show synergistic effect to promote the generation of high density $\text{Ni}_2\text{O}_3\text{-Au}^+$ sites at the interface between NiO and Au particles. By nature, the Ni_2O_3 specimens play a key role not only in promoting the formation of Au^+ and stabilizing them but also in acting as surface-active-oxygen species supplier.

Acknowledgements

We thank the NSF of China (20973063, 21076083, 21273075), the MOST of China (2011CB201403), the Fundamental Research Funds for the Central Universities, the Specialized Research Fund for the Doctoral Program of Higher Education (20090076110006), the Shanghai Rising-Star Program (10QH1400800) and the Shanghai Leading Academic Discipline Project (B409) for their financial support, as well as the Electron Spectroscopy Center of the East China Normal University for providing the TEM measurements.

References

- [1] S. Biella, M. Rossi, *Chem. Commun.* 2003, 378-380.
- [2] A.S.K. Hashmi, G.J. Hutchings, *Angew. Chem. Int. Ed.* 45 (2006) 7896-7936.
- [3] C.D. Pina, E. Falletta, M. Rossi, *J. Catal.* 260 (2008) 384-386.
- [4] A. Corma, H. Garcia, *Chem. Soc. Rev.* 37 (2008) 2096-2126.
- [5] J. P. Mao, M. M. Deng, Q. S. Xue, L. Chen, Y. Lu, *Catal. Commun.* 10 (2009) 1376-1379.
- [6] L. Prati, F. Porta, *Appl. Catal. A-Gen.* 291 (2005) 199-203.
- [7] A. Villa, N. Janjic, P. Spontoni, D. Wang, D.S. Su, L. Prati, *Appl. Catal. A-Gen.* 364 (2009) 221-228.

- [8] F. Li, Q. Zhang, Y. Wang, *Appl. Catal. A-Gen.* 334 (2008) 217-226.
- [9] X. Wang, H. Kawanami, S.E. Dapurkar, N.S. Venkataramanan, M. Chatterjee, T. Yokoyama, Y. Ikushima, *Appl. Catal. A-Gen.* 349 (2008) 86-90.
- [10] M. Haruta, T. Kobayashi, H. Sano, N. Yamada, *Chem. Lett.* 2 (1987) 405-408.
- [11] R. Meyer, C. Lemire, S.K. Shaikhutdinov, H.J. Freund, *Gold Bull.* 37 (2004) 72-124.
- [12] M.S. Chen, D.G. Goodman, *Science* 306 (2004) 252-255.
- [13] A.A. Herzing, C.J. Kiely, A.F. Carley, P. Landon, G.J. Hutchings, *Science* 321 (2008) 1331-1335
- [14] G.C. Bond, D.T. Thompson, *Catal. Rev. Sci. Eng.* 41 (1999) 319-388.
- [15] B.K. Min, C.M. Friend, *Chem. Rev.* 107 (2007) 2709-2724.
- [16] J.C. Fierro-Gonzalez, B.C. Gates, *Chem. Soc. Rev.* 37 (2008) 2127-2134
- [17] P.X. Huang, F. Wu, B.L. Zhu, X.P. Gao, H.Y. Zhu, T.Y. Yan, W.P. Huang, S.H. Wu, D.Y. Song, *J. Phys. Chem. B* 109 (2005) 19169-19174.
- [18] J. Guzman, S. Carrettin, A. Corma, *J. Am. Chem. Soc.* 127 (2005) 3286-3287.
- [19] M. Comotti, W.C. Li, B. Spliethoff, F. Schüth, *J. Am. Chem. Soc.* 128 (2006) 917-924.
- [20] J. Li, N. Ta, Y. Li, W.J. Shen, *Chin. J. Catal.*, 29 (2008) 823.
- [21] R. Si, M. Flytzani-Stephanopoulos, *Angew. Chem. Int. Ed.*, 47 (2008) 2884-2887.
- [22] A. Abad, P. Concepción, A. Corma, H. García, *Angew. Chem. Int. Ed.* 44 (2005) 4066-4069.
- [23] J.A. Rodriguez, S. Ma, P. Liu, J. Hrbek, J. Evans, M. Pérez, *Science* 318 (2007) 1757-1760.
- [24] C.M.Y. Yeung, K.M.K. Yu, Q.J. Fu, D. Thompsett, M.I. Petch, S.C. Tsang, *J. Am. Chem. Soc.* 127 (2005) 18010-18011.
- [25] T. Fujitani, I. Nakamura, T. Akita, M. Okumura, M. Haruta, *Angew. Chem. Int. Ed.* 48 (2009)

9515-9518.

- [26] G.F. Zhao, H.Y. Hu, M.M. Deng, Y. Lu, *Chem. Commun.* 47 (2011) 9642-9644.
- [27] G.F. Zhao, H.Y. Hu, W. Chen, Z. Jiang, S. Zhang, J. Huang, Y. Lu, *Catal. Sci. Technol.* 3 (2013) 404-408.
- [28] G.F. Zhao, M.M. Deng, Y.F. Jiang, H.Y. Hu, J. Huang, Y. Lu, *J. Catal.* 301 (2013) 46-53.
- [29] G.F. Zhao, H.Y. Hu, M.M. Deng, M. Ling, Y. Lu, *Green Chem.* 13 (2011) 55-58.
- [30] G.F. Zhao, H.Y. Hu, M.M. Deng, M. Ling, Y. Lu, *ChemCatChem* 3 (2011) 1629-1636.
- [31] M.M. Deng, G.F. Zhao, Q.S. Xue, L. Chen, Y. Lu, *Appl. Catal. B-Environ.* 99 (2010) 222-228.
- [32] J.P. Mao, M.M. Deng, L. Chen, Y. Liu, Y. Lu, *AIChE J.* 56 (2010) 1545-1556.
- [33] J. Fan, Y.H. Dai, Y.L. Li, N.F. Zheng, J.F. Guo, X.Q. Yan, G.D. Stucky, *J. Am. Chem. Soc.* 131 (2009) 15568-15569.
- [34] J. Guzman, B.C. Gates, *J. Am. Chem. Soc.* 126 (2004) 2672-2673.
- [35] M.K. Oudenhuijzen, J.A. van Bokhoven, J.T. Miller, D.E. Ramaker, D.C. Koningsberger, *J. Am. Chem. Soc.* 127 (2005) 1530-1540.
- [36] J.A. van Bokhoven, C. Louis, J.T. Miller, M. Tromp, O.V. Safonova, P. Glatzel, *Angew. Chem. Int. Ed.* 45 (2006) 4651-4654.
- [37] J.T. Miller, A.J. Kropf, Y. Zha, J.R. Regalbuto, L. Delannoy, C. Louis, E. Bus, J.A. van Bokhoven, *J. Catal.* 240 (2006) 222-234.
- [38] A. Villa, G.M. Veith, D. Ferri, A. Weidenkaff, K.A. Perry, S. Campisia, L. Prati, *Catal. Sci. Technol.* 3 (2013) 394-399.
- [39] A. Trovarelli, *Catal. Rev. Sci. Eng.* 38 (1996) 439-520.
- [40] G. F. Zhao, J. Huang, Z. Jiang, S. Zhang, L. Chen, Y. Lu, *Appl. Catal. B-Environ.* 140-141

(2013) 249-257

Accepted Manuscript

List of Figure Captions:

Fig. 1 (A) SEM image of the Au-5/Ti catalyst; (B) XRD patterns of the Au-5/Ti catalyst and Ti powder; (C) TEM image of the Au-5/Ti catalyst; (D) TEM image of the NiO-1@Au-5/Ti-Cl catalyst.

Fig. 2 XRD patterns of the NiO-1@Au-5/Ti-Cl catalyst with the formation of NiO.

Fig. 3 Influences of NiO and Au loadings on the catalytic performance of the NiO@Au/Ti-Cl catalyst for the gas-phase oxidation of benzyl alcohol at 280 °C using $O_2/\text{hydroxyl} = 0.6$ and $WHSV = 20 \text{ h}^{-1}$. (A) The influence of NiO loading (setting Au loading constant at 5 wt%); (B) The influence of Au loading (setting Au/NiO weight ratio constant at 5). Pre-activated process: the catalysts underwent 1 h reaction in the gas-phase oxidation of benzyl alcohol at 380 °C with $O_2/\text{hydroxyl} = 0.6$ and $WHSV = 20 \text{ h}^{-1}$.

Fig. 4 (A) Longer-term test using a reaction/regeneration cycle for the NiO-1@Au-5/Ti-Cl catalyst in the gas-phase oxidation of benzyl alcohol. Reaction conditions: 280 °C, $O_2/\text{hydroxyl} = 0.6$, $WHSV = 20 \text{ h}^{-1}$. Regeneration conditions: oxidation at 400 °C in air for 3 h to burn off carbon deposits; (B) Longer-term test for the NiO-1@Au-5/Ti-Cl catalyst in the gas-phase oxidation of cyclopropyl carbinol. Reaction conditions: 280 °C, $O_2/\text{hydroxyl} = 0.6$, $WHSV = 20 \text{ h}^{-1}$.

Fig. 5 XPS spectra in O1s, Ni2p, and Au4f regions. Sample a: NiO-1@Au-5/Ti-Cl reacting with benzyl alcohol at 280 °C for 0.5 h in the present of O_2 . Benzyl alcohol conversion = 94%; Sample b: Sample a after switching off the O_2 feed followed by a 15 min reaction with benzyl alcohol alone at 280 °C. Benzyl alcohol conversion = 2%; Sample c: Sample b catalyzing benzyl alcohol oxidation by re-feeding O_2 again under the same conditions as for the sample a for 10 min. Benzyl alcohol conversion = 88%.

Fig. 6 XANES of Au L₃-edge (A) and Modulus of the Fourier-transform Au L₃-edge signal (B) of several catalysts: (a) sample a as in Fig. 5-a; (b) Au foil; (c) sample b as in Fig. 5-b; (d) sample c as in Fig. 5-c.

Fig. 7 Ni K-edge XANES (A) and modulus of the Fourier-transform of Ni K edge signal (B) of several catalysts. (a) Ni₂O₃; (b) sample a as in Fig. 5-a; (c) sample b as in Fig. 5-b; (d) sample c as in Fig. 5-c; (e) NiO.

Table 1 Gas-phase oxidation of benzyl alcohol catalyzed by various designed catalysts.

Entry	Catalyst ^{a,b,c}	D _{Au} ^d (nm)	T _{React.} (°C)	Conversion (%)	Selectivity ^f (%)
1	Ti-powder	-	280	0	0
2	Au-5/Ti	35	280	5.0	99.7
3	NiO-1@Au-5/Ti-Cl	33	280	93.7	98.5
4	NiO-1/Ti-Cl	-	280	2.3	99.8
5	Au-5@NiO-1/Ti-Cl	33	280	21.1	98.9
6	NiO-1@Au-5/Ti-C	34	280	92.1	98.4
7	NiO-1@Au-5/Ti-N	34	280	94.6	98.5
8	NiO-1@Au-5/Ti-N	34	260	89.1	98.6
9	NiO-1@Au-5/Ti-N	34	240	87.2	98.6
10	NiO-1@Au-5/Ti-N	34	230	86.0	98.9
11	NiO-1@Au-5/Ti-N	34	220	63.5	99.2
12	Au-5/Ti&NiO-1/Ti-Cl ^e	34	280	4.3	99.6

^a The Au loading was 5 wt% and NiO loading (if has) was 1 wt%; see experimental section for detailed catalyst preparation; ^b The catalysts were all pre-activated over the gas-phase oxidation of benzyl alcohol at 380 °C for 1 h using the molar ratio of O₂ to alcoholic hydroxyl (O₂/hydroxyl) = 0.6 and weight hourly space velocity (WHSV) = 20 h⁻¹, and then evaluated at 220-280 °C with other reaction parameters unchanged; ^c To represent different nickel precursors: Cl-NiCl₂, C-Ni(Ac)₂, N-Ni(NO₃)₂; ^d The particle size was estimated from the XRD patterns using Scherrer's equation. ^e The physical mixture of the catalysts Au-5/Ti and NiO-1/Ti-Cl (mass ratio, 50:50). ^f The byproducts are CO, CO₂, benzene, toluene and benzoic acid in traces, whose total selectivity is 1.0-1.5%.

Table 2. Oxidation of various alcohols over the NiO-1@Au-5/Ti-Cl catalyst using WHSV of 20 h⁻¹.

Substrate	O ₂ /hydroxyl (mol/mol)	T _{React.} (°C)	Conversion (%)	Selectivity (%)
1-phenylethanol	0.7	300	95.3	98.3
2-phenylethanol	0.7	340	51.2	98.1
1-octanol	0.6	300	51.9	92.5
2-octanol	0.6	360	23.4	66.9
Cyclohexanol	0.6	340	67.8	97.4
1,2-propanediol	0.7	360	91.6	71.0

Table 3. The XPS results of the NiO-1@Au-5/Ti-Cl samples.

Elements		B.E. (eV)	Fraction (%)		
			Sample a ^a	Sample b ^b	Sample c ^c
Au	Au ⁰	84.0	63.0	96.6	67.0
	Au ⁺	84.7	37.0	3.4	33.0
Ni	NiO	854.4	23.0	40.0	27.0
	Ni ₂ O ₃	856.2	77.0	60.0	73.0
O	NiO	529.2	11.0	20.0	13.0
	Ni ₂ O ₃	532.1	53.0	44.0	51.0
	TiO ₂	530.4	36.0	36.0	36.0

^a Sample a: NiO-1@Au-5/Ti-Cl reacting with benzyl alcohol at 280 °C in the presence of O₂ for 0.5 h. Benzyl alcohol conversion = 94%; ^b Sample b: Sample a after switching off the O₂ feed followed by a 15 min reaction with benzyl alcohol alone at 280 °C. Benzyl alcohol conversion = 2%; ^c Sample c: Sample b catalyzing benzyl alcohol oxidation by re-feeding O₂ again under the same conditions as for sample a for 10 min. Benzyl alcohol conversion = 88%.

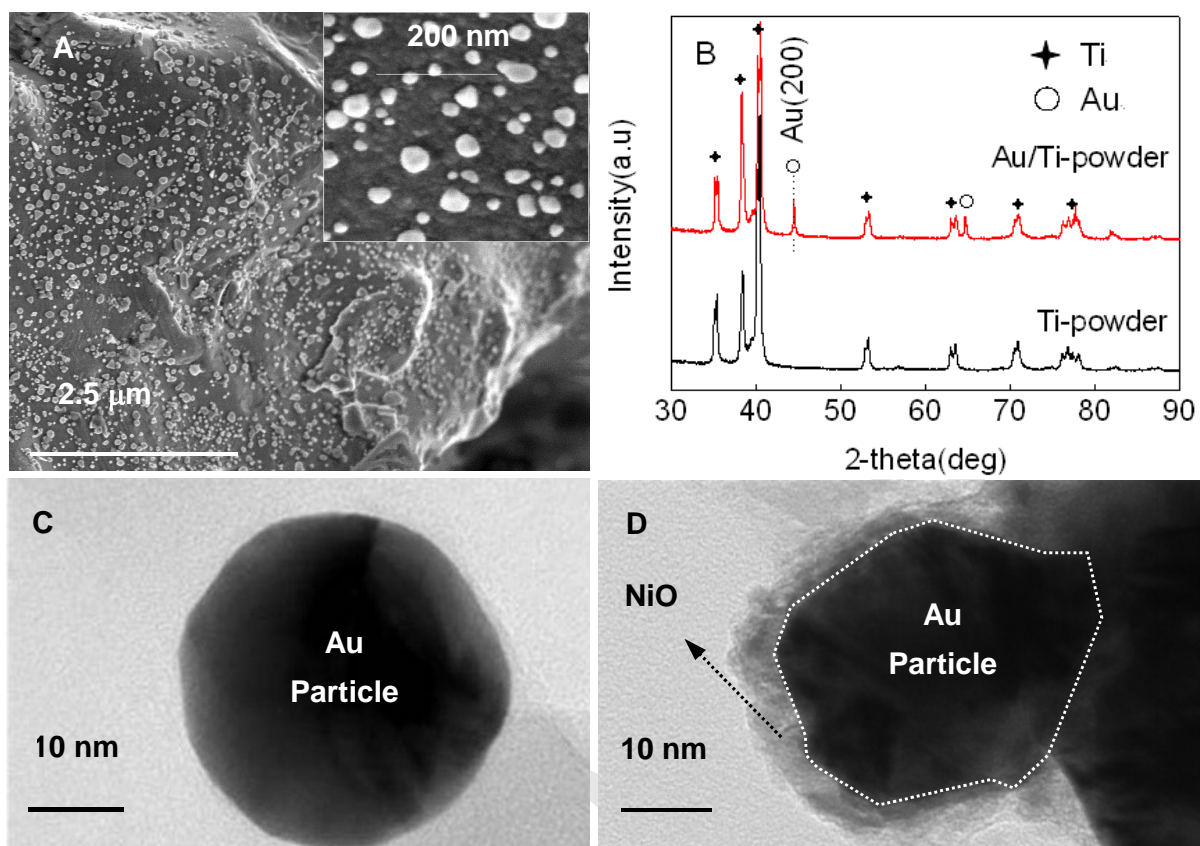


Fig. 1 (A) SEM image of the Au-5/Ti catalyst; (B) XRD patterns of the Au-5/Ti catalyst and Ti powder; (C) TEM image of the Au-5/Ti catalyst; (D) TEM image of the NiO-1@Au-5/Ti-Cl catalyst.

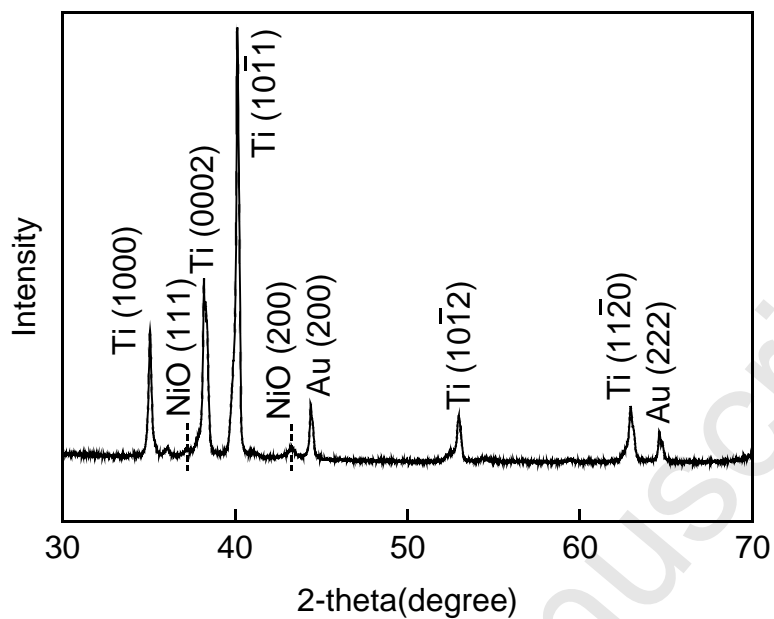


Fig. 2 XRD patterns of the NiO-1@Au-5/Ti-Cl catalyst with the formation of NiO.

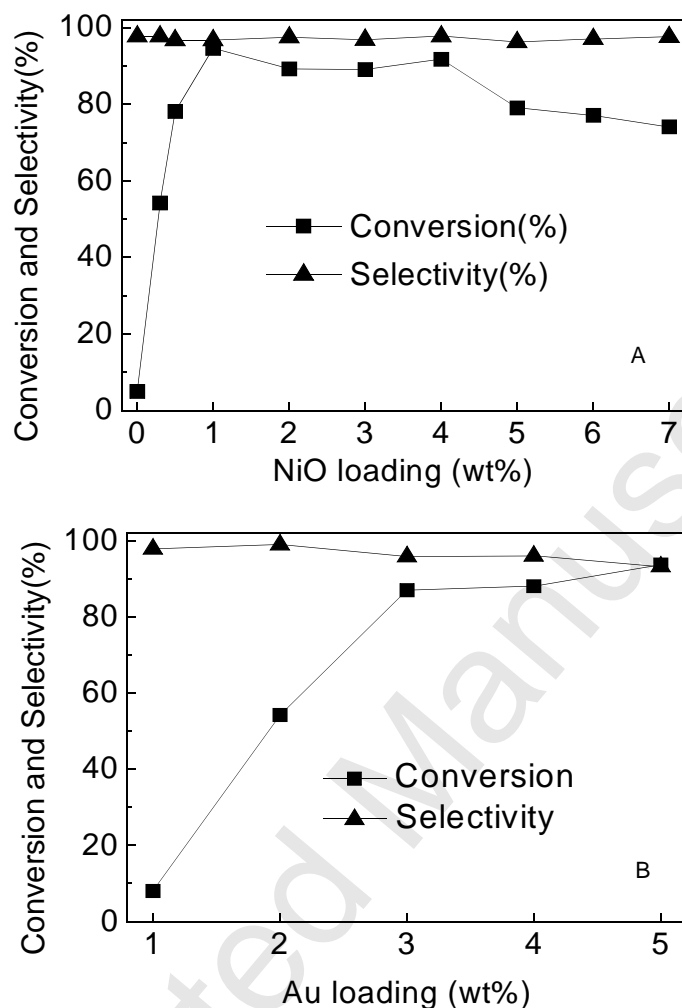


Fig. 3 Influences of NiO and Au loadings on the catalytic performance of the NiO@Au/Ti-Cl catalyst for the gas-phase oxidation of benzyl alcohol at 280 °C using $O_2/\text{hydroxyl} = 0.6$ and $WHSV = 20 \text{ h}^{-1}$. (A) The influence of NiO loading (setting Au loading constant at 5 wt%); (B) The influence of Au loading (setting Au/NiO weight ratio constant at 5). Pre-activated process: the catalysts underwent 1 h reaction in the gas-phase oxidation of benzyl alcohol at 380 °C with $O_2/\text{hydroxyl} = 0.6$ and $WHSV = 20 \text{ h}^{-1}$.

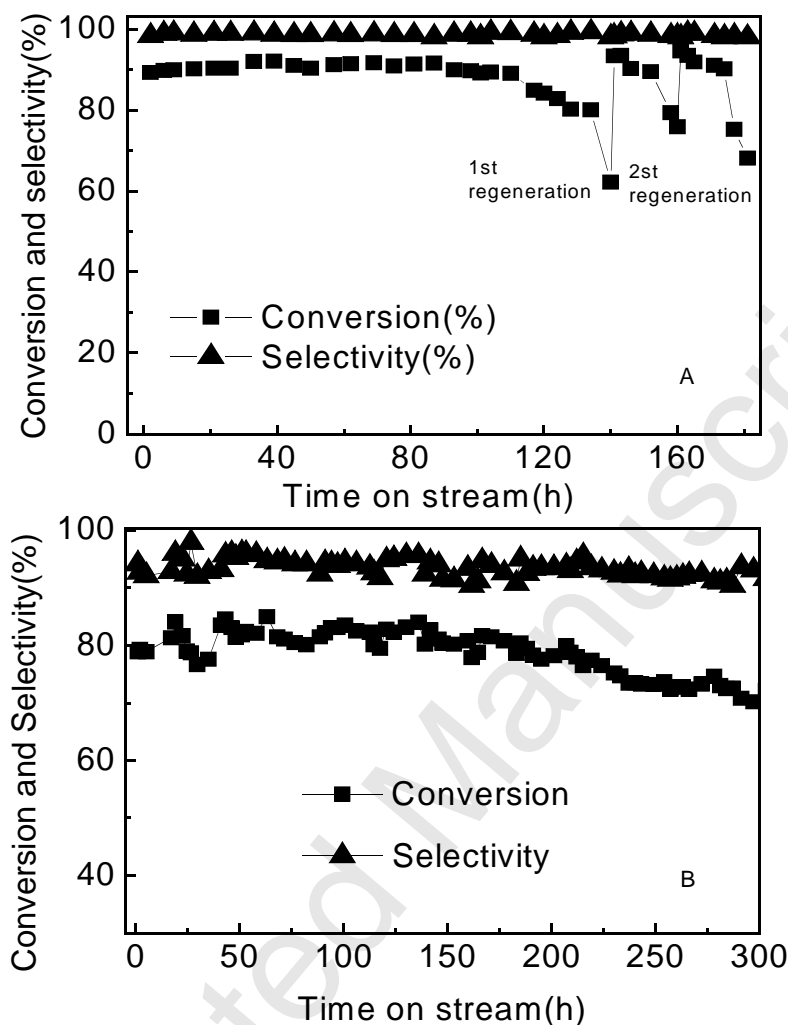


Fig. 4 (A) Longer-term test using a reaction/regeneration cycle for the NiO-1@Au-5/Ti-Cl catalyst in the gas-phase oxidation of benzyl alcohol. Reaction conditions: 280 °C, $O_2/\text{hydroxyl} = 0.6$, $WHSV = 20 \text{ h}^{-1}$. Regeneration conditions: oxidation at 400 °C in air for 3 h to burn off carbon deposits; (B) Longer-term test for the NiO-1@Au-5/Ti-Cl catalyst in the gas-phase oxidation of cyclopropyl carbinol. Reaction conditions: 280 °C, $O_2/\text{hydroxyl} = 0.6$, $WHSV = 20 \text{ h}^{-1}$.

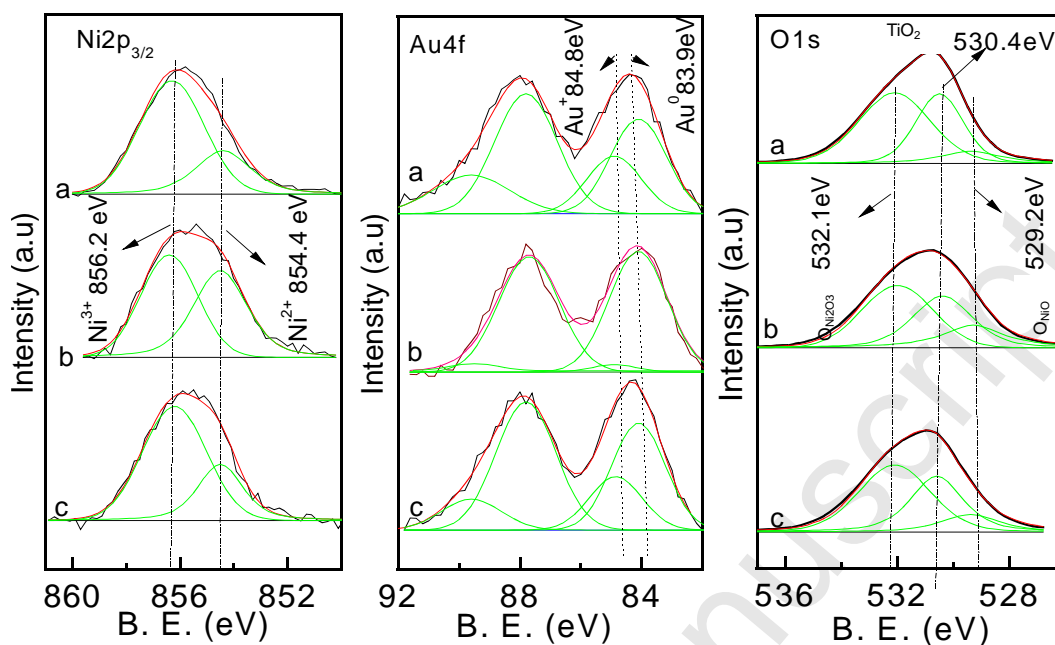


Fig. 5 XPS spectra in O1s, Ni2p, and Au4f regions. Sample a: NiO-1@Au-5/Ti-Cl reacting with benzyl alcohol at 280 °C in the present of O₂ for 0.5 h. Benzyl alcohol conversion = 94%; Sample b: Sample a after switching off the O₂ feed followed by a 15 min reaction with benzyl alcohol alone at 280 °C. Benzyl alcohol conversion = 2%; Sample c: Sample b catalyzing benzyl alcohol oxidation by re-feeding O₂ again under the same conditions as for sample a for 10 min. Benzyl alcohol conversion = 88%.

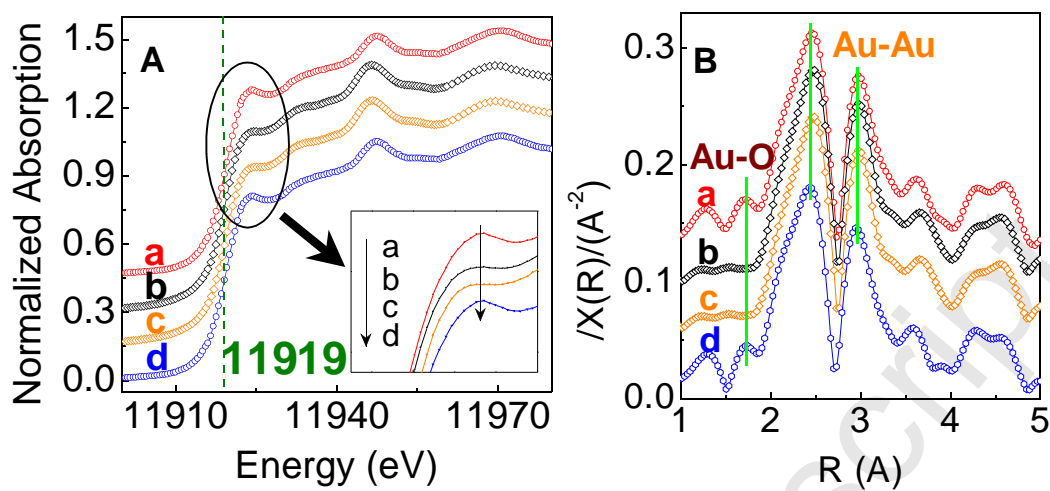


Fig. 6 XANES of Au L₃-edge (A) and Modulus of the Fourier-transform Au L₃-edge signal (B) of several catalysts: (a) sample a as in Fig. 5-a; (b) Au foil; (c) sample b as in Fig. 5-b; (d) sample c as in Fig. 5-c.

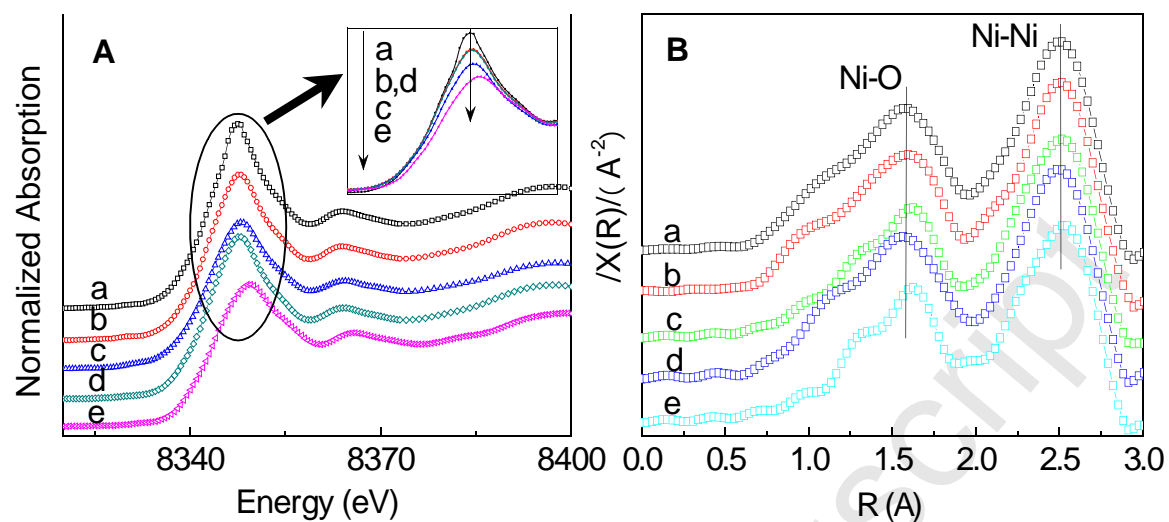
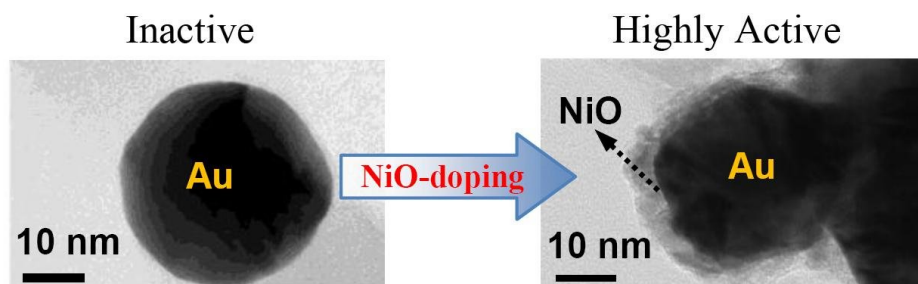


Fig. 7 Ni K-edge XANES (A) and modulus of the Fourier-transform of Ni K edge signal (B) of several catalysts. (a) Ni₂O₃; (b) sample a as in Fig. 5-a; (c) sample b as in Fig. 5-b; (d) sample c as in Fig. 5-c; (e) NiO.

Graphical abstract



Highlights

NiO-doped Au/Ti-powder catalyst is highly active for gas-phase oxidation of alcohols.

The catalyst shows good stability in longer-term test of alcohol oxidation.

Formation of the NiO@Au ensembles is essential to the high activity.

Ni₂O₃-Au⁺ was defined as active-site for the selective oxidation of alcohol.

Accepted Manuscript